

Recent results on reactions with radioactive beams at RIBRAS (Radioactive Ion Beams in Brazil)

A Lépine-Szily¹, R Lichtenthäler¹, V Guimarães¹, A Arazi², A Barioni^{1,3}, E A Benjamim¹, P N de Faria^{1,4}, P Descouvemont⁵, L R Gasques¹, E Leistenschneider^{1,6}, D R Mendes Jr⁴, M C Morais^{1,4}, V Morcelle¹, A M Moro⁷, R Pampa Condori¹, K C C Pires¹, M Rodriguez-Gallardo⁷, V Scarduelli¹, J M B Shorto⁸, J C Zamora^{1,9}

¹ Instituto de Física, Universidade de São Paulo, CP 66318, 05389-970, São Paulo, Brazil

² Laboratorio Tandar, Departamento de Física, Comisión Nacional de Energía Atómica, Av. del Libertador 8250, (1429), Buenos Aires, Argentina

³ Instituto de Física, Universidade Federal da Bahia, 40210-340, Bahia, Brazil

⁴ Instituto de Física - Universidade Federal Fluminense, Niterói, R.J., 24210-340, Brazil

⁵ Physique Nucléaire Théorique et Physique Mathématique, C.P. 229, Université Libre de Bruxelles (ULB), B 1050 Brussels, Belgium

⁶ TRIUMF, V6T2A3 Vancouver B. C., Canada

⁷ Departamento de FAMN, Universidad de Sevilla, Apto. 1065, E-41080 Seville, Spain

⁸ Instituto de Pesquisas Energéticas e Nucleares, Av. Prof. Lineu Prestes 2242, São Paulo, Brasil

⁹ Technische Universität Darmstadt, Germany

E-mail: alinka@if.usp.br

Abstract. We present a quick description of RIBRAS (Radioactive Ion beams in Brazil), which is a superconducting double solenoid system, installed at the Pelletron Laboratory of the University of São Paulo and extends the capabilities of the original Pelletron Tandem Accelerator of 8MV terminal voltage (8UD) by producing secondary beams of unstable nuclei. The experimental program of the RIBRAS covers the study of elastic and inelastic scattering with the objective to study the interaction potential and the reaction mechanisms between weakly bound (RIB) and halo (⁶He and ⁸B) projectiles on light, medium and heavy mass targets. With highly purified beams, the study of resonant elastic scattering and resonant transfer reactions, using inverse kinematics and thick targets, have also been included in our recent experimental program.

1. Introduction

Great progress in our understanding of nuclear structure is due to experiments performed in many laboratories using radioactive ion beams (RIB). Before the use of RIB, knowledge of nuclear structure and reactions was based on experiments using systems of stable or very long lived nuclei. However, more than 90% of all nuclei, most of them still unknown, are located between the stability line and the drip lines, where many new phenomena can take place.

The use of transfer reactions to produce RIB is possible at quite low energies ($E \leq 10\text{MeV/n}$) and, in this way, small university laboratories can also make important contributions in this field. Their main advantage is that they produce low energy RIB. At energies near the Coulomb



barrier or above, valuable information on the structure of exotic nuclei and on the dynamics of the nuclear reactions between them can be obtained. Important issues, such as fusion below the Coulomb barrier, and the role of the neutron halo with respect to fusion, can be studied only with low energy beams. Many experiments were performed with light exotic nuclei presenting halo, such as ^6He , ^8He , ^{11}Li , or ^{11}Be among others [1]. On the other hand, recent experiments with radioactive ion beams have been very successful in nuclear astrophysics investigations, where many stellar scenarios involve short-lived nuclei [2]. In this paper we intend to give a short description of the experimental device [3, 4] and of the scientific results achieved recently.

2. Experimental devices and method

The RIBRAS system consists of two superconducting solenoids of 6.5 T maximum central field (5 Tm axial field integral)[5]. The production system (primary target) can be a gas or a solid target, such as a ^9Be foil, mounted before the first solenoid. The primary beam, but also the secondary beams, in the angular range between zero and 2° , are stopped and collected by a tungsten rod with electron and geometrical suppression (Faraday cup), located downstream after the production target. A collimator at the entrance of the first solenoid limits the maximum angular acceptance to 6° , so, in this set-up, the angular divergence of the secondary beams entering the first solenoid is 4° , between 2° and 6° . The angular divergence of the secondary beam in central chamber is 3.2° , between 1.3° and 4.5° .



Figure 1. The RIBRAS facility. The stable beam comes from the left, the production target is located on the left side of the first solenoid. Between the two solenoids one can see the intermediate scattering chamber. At the right extremity, after the second solenoid, the new, large scattering chamber can be seen. Taken from reference [3].

The first solenoid makes an in-flight selection by the magnetic rigidity of the reaction products emerging from the primary target in the forward angle region. As the first magnet focuses all ions with the same magnetic rigidity, i.e., the same ME/Q^2 ratio, where M , E and Q stand for mass, energy, and charge state of the ion, the beam of interest can be accompanied by many contaminant beams of the same magnetic rigidity, but with different charges, masses and energies.

Table 1. Secondary beams produced at the RIBRAS facility and the nuclear reactions used for their production. The intensities, energy resolution (FWHM) and energies obtained for the beams at the central chamber are also shown. The intensities are reported in *pps* per $1\mu\text{A}$ of primary beam.

Secondary beam	Production reaction	Q-value (MeV)	intensity (pps)	Energy resolution FWHM(keV)/Energy
${}^6\text{He}$	${}^9\text{Be}({}^7\text{Li}, {}^6\text{He}){}^{10}\text{B}$	-3.390	$10^5 - 10^6$	1000/22 MeV
${}^7\text{Be}$	${}^3\text{He}({}^6\text{Li}, {}^7\text{Be})\text{d}$	+0.112	$10^4 - 10^5$	800/18.8 MeV
${}^7\text{Be}$	${}^7\text{Li}({}^6\text{Li}, {}^7\text{Be}){}^6\text{He}$	-4.369	$10^4 - 10^5$	1000/22 MeV
${}^8\text{Li}$	${}^9\text{Be}({}^7\text{Li}, {}^8\text{Li}){}^8\text{Be}$	+0.367	$10^5 - 10^6$	500/25.8 MeV
${}^8\text{B}$	${}^3\text{He}({}^6\text{Li}, {}^8\text{B})\text{n}$	-1.975	10^4	1000/15.6 MeV
${}^{10}\text{Be}$	${}^9\text{Be}({}^{11}\text{B}, {}^{10}\text{Be}){}^{10}\text{B}$	-4.642	10^5	800/23.2 MeV
${}^{12}\text{B}$	${}^9\text{Be}({}^{11}\text{B}, {}^{12}\text{B}){}^8\text{Be}$	+1.705	10^5	800/25.0 MeV

3. Elastic scattering of 2-n halo projectile ${}^6\text{He}$: Experimental results and analysis

Until recently almost all experiments performed at RIBRAS were on elastic scattering using only the first solenoid. Elastic scattering angular distributions were measured for the available radioactive beams (${}^6\text{He}$, ${}^8\text{Li}$, ${}^7, {}^{10}\text{Be}$ and ${}^8\text{B}$) on light, medium mass and heavy targets at various energies, near and above the Coulomb barrier [4, 6–17]. The ${}^6\text{He}$ and ${}^8\text{Li}$ secondary beams were produced respectively by the one-proton and one-neutron transfer reactions, ${}^9\text{Be}({}^7\text{Li}, {}^6\text{He}){}^{10}\text{B}$ ($Q = -3.39$ MeV) and ${}^9\text{Be}({}^7\text{Li}, {}^8\text{Li}){}^8\text{Be}$ ($Q = 0.3677$ MeV), using the ${}^7\text{Li}$ primary beam accelerated by the Pelletron tandem and a ${}^9\text{Be}$ target. A central scattering chamber, located between the two solenoids, was used and the reaction products were detected using ΔE -E Si telescopes, with detector thicknesses of 20 - 500 (or 1000) μm respectively.

These measurements are important since they allow the determination of the optical potentials between the radioactive projectiles and the targets. The elastic scattering also gives information on the total reaction cross section and on the size of the nuclei involved. The coupling of the elastic scattering to other important channels, as breakup or transfer, can also be investigated through the elastic scattering experiments. In the case of radioactive projectiles, these effects are strongly enhanced and their study as a function of the target mass or the incident energy was achieved by our measurements.

We have measured the elastic scattering of the 2-neutron halo projectile ${}^6\text{He}$, on ${}^9\text{Be}$, ${}^{27}\text{Al}$, ${}^{51}\text{V}$, ${}^{58}\text{Ni}$ and ${}^{120}\text{Sn}$ targets at energies around and above the Coulomb barrier. The data on ${}^{27}\text{Al}$, ${}^{51}\text{V}$ were analyzed using optical model and the "São Paulo optical potential" [18, 19]. The normalization of the imaginary part N_I and the diffuseness, a , of the projectile were adjusted to reproduce the data [16, 20]. For ${}^6\text{He} + {}^{51}\text{V}$ at 23.0 and 15.4 MeV, both N_I and a had to be increased, when compared to typical, strongly bound, stable nuclei, indicating a larger absorption. This feature is different from the ${}^6\text{He} + {}^{27}\text{Al}$ case [16], where the N_I and a values were similar to the values used for typical, strongly bound, stable nuclei, respectively, $N_I = 0.78$ and $a = 0.56(2)\text{fm}$.

For the systems with ${}^6\text{He}$ projectile, on ${}^9\text{Be}$, ${}^{58}\text{Ni}$ and ${}^{120}\text{Sn}$ targets, the elastic scattering angular distributions were compared to Continuum Discretized Coupled Channels (CDCC) calculations [21]. CDCC has been applied to a number of cases in recent years, first for the three-body problem [22–26] where the projectile is considered as a core plus a valence particle. In the three-body model, the ${}^6\text{He}$ structure is simplified to an alpha-particle core plus a di-neutron which means that the neutron pair is treated as a single particle bound to the alpha core by 0.973 MeV. More recently, full four-body calculations [27–30], applied to the problem of

2-neutron halo projectiles as ${}^6\text{He}$, were also realized.

In Figure 2 we present an example of our data compared to CDCC calculations [6, 9]. For the ${}^6\text{He}+{}^{58}\text{Ni}$ system (Figure 2) the elastic scattering angular distribution is compared with no-continuum CDCC, three, and four-body CDCC calculations, considering projectile breakup [6]. The agreement between the four-body CDCC and the experimental data is remarkable in the whole angular range.

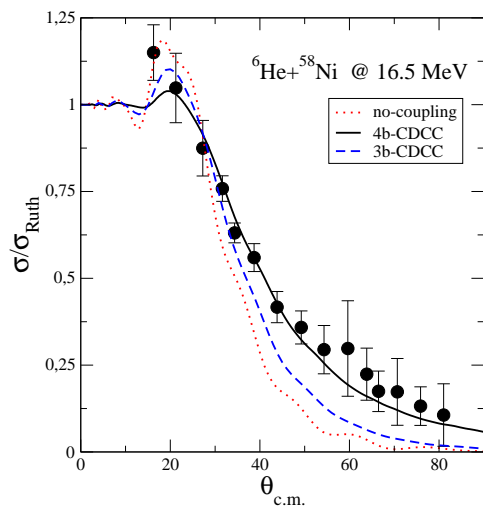


Figure 2. Angular distribution of ${}^6\text{He}+{}^{58}\text{Ni}$ elastic scattering. The experimental angular distribution is compared to calculations: red dotted curve is without coupling to the continuum, blue dashed curve is 3b-CDCC calculation and the black solid line is the 4b-CDCC. Taken from ref. [6].

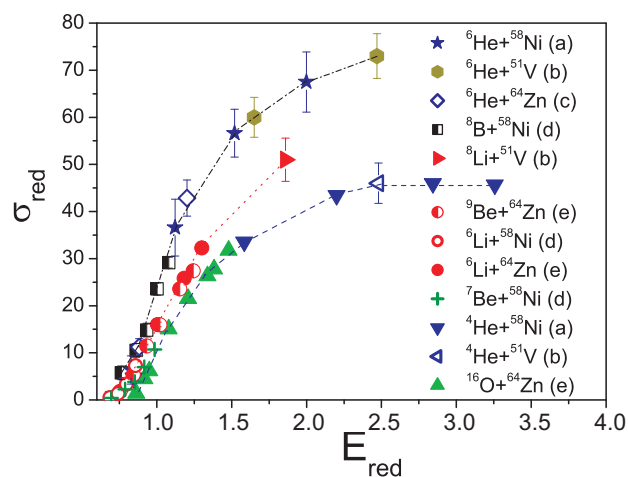


Figure 3. Reduced reaction cross sections for different projectiles on intermediate mass ($A \approx 60$) targets: Ref. (a) from [6, 31, 32], (b) from [20], (c) from [33], (d) from [34] and (e) from [35–37]. The units of σ_{red} and E_{red} are, respectively, mb and MeV. The lines are to guide the eye. Taken from ref. [4].

The total reaction cross section can also be obtained from the experimental data of elastic scattering or from the optical model or CDCC calculations used to reproduce the elastic data. Comparing total reaction cross sections for different systems can be an interesting way to investigate the influence or competition of reaction mechanisms, such as breakup, transfer, and fusion. This can be particularly revealing, if these systems have weakly bound or exotic projectiles. In order to compare total reaction cross sections for systems of different masses and charges at different energies, it is necessary to use a scaling procedure [35, 38–40] to remove trivial effects due to different sizes and energies with respect to the Coulomb barriers.

We present on Fig.3 the reduced reaction cross sections for different projectiles on intermediate mass ($A \approx 60$) targets. We see three bands, the one with lowest reduced reaction cross section corresponds to tightly bound, α -cluster (${}^{16}\text{O}$ and ${}^4\text{He}$) projectiles on ${}^{64}\text{Zn}$ and ${}^{58}\text{Ni}$ targets, respectively. The one with the highest reduced reaction cross section corresponds to exotic halo nuclei, ${}^6\text{He}$ and ${}^8\text{B}$, on ${}^{64}\text{Zn}$, ${}^{51}\text{V}$, and ${}^{58}\text{Ni}$ targets. The band between both corresponds to reactions of weakly bound, stable (${}^6\text{Li}$ and ${}^9\text{Be}$) and radioactive (${}^8\text{Li}$ and ${}^7\text{Be}$) projectiles. A strong enhancement is observed in the total reaction cross section of the exotic ${}^6\text{He}$ projectile compared with tightly bound and weakly bound stable systems, probably due to

the coupling to Coulomb break up.

4. Scattering on hydrogen target: $^8\text{Li} + p$ excitation functions

The use of two magnets in RIBRAS is important to purify the secondary beams. With two solenoids, it is possible to use the differential energy loss in an energy degrader foil, located at the crossover point between the magnets, to select the ion of interest and move the contaminant ions out of the band pass of the second solenoid. The $^8\text{Li}(p,p)^8\text{Li}$ measurement was performed in the large scattering chamber located after the second solenoid with a nearly pure (95-99%) ^8Li beam on the secondary target of a proton-rich $[\text{CH}_2]_n$ polyethylene foil of 7.7 mg/cm^2 thickness. The $^8\text{Li}(p,p)^8\text{Li}$ elastic scattering excitation function and the $^8\text{Li}(p,d)^7\text{Li}$ and $^8\text{Li}(p,\alpha)^5\text{He}$ reactions could also be observed in this experiment [41]. The excitation functions are shown in Figure 4 together with R-matrix calculations [42, 43]. With the R-matrix fits we could determine, or at least constrain, values of spins, parities, total and partial widths (Γ_p , Γ_α and Γ_d) for three resonances, located at $E_{cm} = 1.13$, 1.69 and 1.76 MeV.

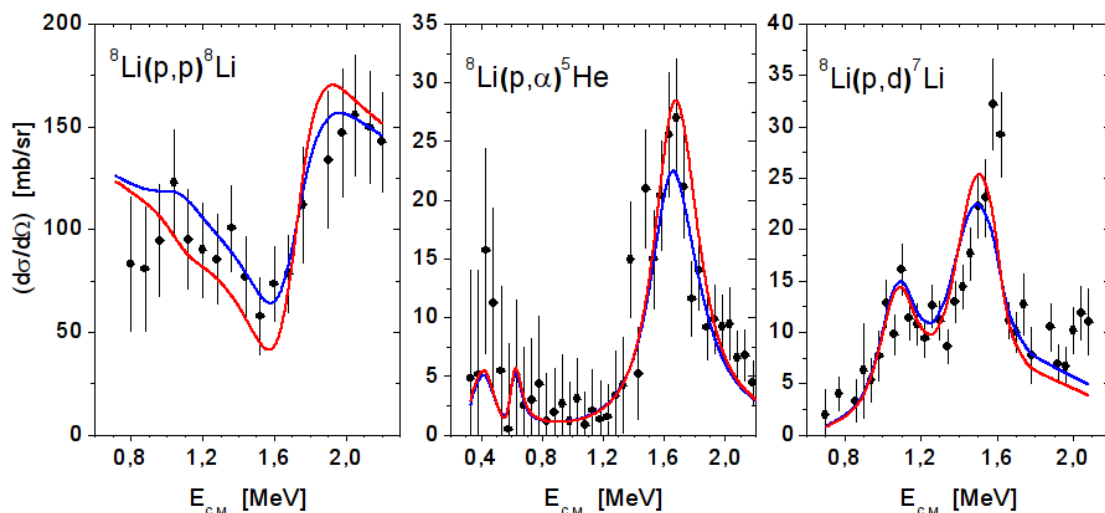


Figure 4. Excitation functions for the elastic scattering $^8\text{Li}(p,p)^8\text{Li}$ and for the reactions $^8\text{Li}(p,\alpha)^5\text{He}$ and $^8\text{Li}(p,d)^7\text{Li}$ with R-matrix calculations [41]. The blue and red curves are best fits with somewhat different parameters

5. Acknowledgements

The authors thank the Fundação de Amparo à Pesquisa do Estado de São Paulo (FAPESP) and the Conselho Nacional de Desenvolvimento Científico e Tecnológico (CNPq) for financial support.

References

- [1] Keeley N, Alamanos N, Kemper K W and Rusek K 2009 *Progr. Part. Nucl. Phys.* **63** 396 – 447
- [2] Langanke K and Wiescher M 2001 *Rep. Prog. Phys.* **64** 1657
- [3] Lépine-Szily A, Lichtenthäler R and Guimarães V 2013 *Nucl. Phys. News* **23**(3) 5–11
- [4] Lépine-Szily A, Lichtenthäler R and Guimarães V 2014 *Eur. Phys. J. A* **50** 128–163
- [5] Lichtenthäler R, Lépine-Szily A, Guimarães V, Perego C, Placco V, Camargo O, Denke R, de Faria P N, Benjamim E A, Added N, Lima G F, Hussein M S, Kolata J J and Arazi A 2005 *Eur. Phys. Jour. A* **25** 733–736

- [6] Morcelle V, Pires K C C, Rodríguez-Gallardo M, Lichtenthäler R, Lépine-Szily A, Guimarães V, de Faria P N, Mendes Jr D R, Moro A M, Gasques L R, Leistenschneider E, Pampa Condori R, Scarduelli V, Morais M C, Barioni A, Zamora J C and Shorto J M B 2014 *Phys. Lett. B* **732** 228
- [7] Mendes D R, Lépine-Szily A, Descouvemont P, Lichtenthäler R, Guimarães V, de Faria P N, Barioni A, Pires K C C, Morcelle V, Pampa Condori R, Morais M C, Leistenschneider E, Lima C E F, Zamora J C, Alcantara J A, Zagatto V, Assunção M and Shorto J M B 2012 *Phys. Rev. C* **86**(6) 064321
- [8] Zamora J C, Guimarães V, Barioni A, Lépine-Szily A, Lichtenthäler R, de Faria P N, Mendes D R, Gasques L R, Shorto J M B, Scarduelli V, Pires K C C, Morcelle V, Leistenschneider E, Condori R P, Zagatto V A, Morais M C and Crema E 2011 *Phys. Rev. C* **84** 034611
- [9] Pires K C C, Lichtenthäler R, Lépine-Szily A, Guimarães V, de Faria P N, Barioni A, Mendes Junior D R, Morcelle V, Pampa Condori R, Morais M C, Zamora J C, Crema E, Moro A M, Rodríguez-Gallardo M, Assuncao M, Shorto J M B and Mukherjee S 2011 *Phys. Rev. C* **83** 064603
- [10] de Faria P N, Lichtenthäler R, Pires K C C, Moro A M, Lépine-Szily A, Guimarães V, Mendes D R, Arazi A, Barioni A, Morcelle V and Morais M C 2010 *Phys. Rev. C* **82** 034602
- [11] de Faria P N, Lichtenthäler R, Pires K C C, Moro A M, Lépine-Szily A, Guimarães V, Mendes D R, Arazi A, Rodríguez-Gallardo M, Barioni A, Morcelle V, Morais M C, Camargo O, Alcantara Nuñez J and Assunção M 2010 *Phys. Rev. C* **81** 044605
- [12] Mukherjee S, Deshmukh N N, Guimarães V, Lubian J, Gomes P R S, Barioni A, Appannababu S, Lopes C C, Cardozo E N, Pires K C C, Lichtenthäler R, Lépine-Szily A, Monteiro D S, Shorto J M B, de Faria P N, Crema E, Morcelle V, Morais M C and Condori R P 2010 *Eur. Phys. Jour. A* **45** 23–28
- [13] Barioni A, Guimarães V, Lépine-Szily A, Lichtenthäler R, Mendes Jr D R, Crema E, Pires K C C, Morais M C, Morcelle V, de Faria P N, Condori R P, Moro A M, Monteiro D S, Shorto J M B, Lubian J and Assunção M 2009 *Phys. Rev. C* **80** 034617
- [14] Lichtenthäler R, de Faria P N, Lépine-Szily A, Guimarães V, Camargo Jr O, Denke R, Benjamim E A, Barioni A, Pires K C C, Mendes D J, Assuncao M, Arazi A, Padron I and Gomes P R S 2007 *Eur. Phys. Jour.-Spec. Top.* **150** 27–30
- [15] Lépine-Szily A, Lichtenthäler R and RIBRAS collaboration 2007 *Nucl. Phys. A* **787** 94C–101C
- [16] Benjamim E A, Lépine-Szily A, Mendes Jr D R, Lichtenthäler R, Guimarães V, Gomes P R S, Chamon L C, Hussein M S, Moro A M, Arazi A, Padron I, Nunez J A, Assuncao M, Barioni A, Camargo Jr O, Denke R Z, de Faria P N and Pires K C C 2007 *Phys. Lett. B* **647** 30–35
- [17] Pires K C C, Lichtenthäler R, Lepine-Szily A and Morcelle V 2014 *Phys. Rev. C* **90** 027605
- [18] Chamon L C, Carlson B V, Gasques L R, Pereira Det al., 2002 *Phys. Rev. C* **66** 014610
- [19] Alvarez M A G, Chamon L C, Hussein M S, Pereira D, Gasques L R, Rossi E S and Silva C P 2003 *Nucl. Phys. A* **723** 93 – 103
- [20] Morcelle V 2007 *Master's Thesis* IFUSP
- [21] Austern N, Iseri Y, Kamimura M, Kawai M, Rawitscher G and Yahiro M 1987 *Phys. Rep.* **154** 125 – 204
- [22] Aguilera E F, Kolata J J, Nunes F M, Becchetti F D et al, 2000 *Phys. Rev. Lett.* **84** 5058–5061
- [23] Aguilera E F, Kolata J J, Becchetti F D et al., 2001 *Phys. Rev. C* **63** 061603
- [24] Keeley N, Cook J M, Kemper K W, Roeder B T, Weintraub W D et al. et al. 2003 *Phys. Rev. C* **68** 054601
- [25] Kakuee O R, Rahighi J, Sánchez-Benitez A M et al., 2003 *Nucl. Phys. A* **728** 339 – 349
- [26] Hussein M S, Lichtenthäler R, Nunes F M and Thompson I J 2006 *Phys. Lett. B* **640** 91 – 95
- [27] Thompson I J 1998 *Comp. Phys. Rep.* **17** 167
- [28] Matsumoto T, Egami T, Ogata K, Iseri Y, Kamimura M and Yahiro M 2006 *Phys. Rev. C* **73** 051602
- [29] Rodríguez-Gallardo M, Arias J M, Gómez-Camacho J et al., 2008 *Phys. Rev. C* **77** 064609
- [30] Rodríguez-Gallardo M, Arias J M, Gómez-Camacho J, Moro A M et al., 2009 *Phys. Rev. C* **80** 051601
- [31] Gasques L R, Chamon L C, Pereira D, Alvarez M A G, Rossi E S et al., 2003 *Phys. Rev. C* **67** 067603
- [32] Gasques L R, Chamon L C, Gomes P R S and Lubian J 2006 *Nucl. Phys. A* **764** 135 – 148
- [33] Di Pietro A, Figuera P, Amorini F et al., 2003 *Europhys. Lett.* **64** 309
- [34] Aguilera E F, Martinez-Quiroz E, Lizcano D et al., 2009 *Phys. Rev. C* **79** 021601
- [35] Gomes P R S, Padron I, Rodriguez M D, Marti G V et al., 2004 *Phys. Lett. B* **601** 20 – 26
- [36] Moraes S B, Gomes P R S, Lubian J, Alves J J S, Anjos R M, Sant'Anna M M, Padrón I, Muri C, Liguori Neto R and Added N 2000 *Phys. Rev. C* **61** 064608
- [37] Gomes P R S, Rodríguez M D, Martí G V et al., 2005 *Phys. Rev. C* **71** 034608
- [38] Gomes P R S, Lubian J, Padron I and Anjos R M 2005 *Phys. Rev. C* **71**(1) 017601
- [39] Canto L F, Gomes P R S, Lubian J, Chamon L C and Crema E 2009 *Nucl. Phys. A* **821** 51 – 71
- [40] Shorto J M B, Gomes P R S, Lubian J, Canto L F, Mukherjee S et al, 2009 *Phys. Lett. B* **678** 77
- [41] Leistenschneider E 2014 *Master's thesis* IFUSP
- [42] Lane A M and Thomas R G 1958 *Rev. Mod. Phys.* **30** 257
- [43] Descouvemont P and Baye D 2010 *Rep. Prog. Phys.* **73** 036301